We are IntechOpen, the world's leading publisher of Open Access books Built by scientists, for scientists

4,800
Open access books available

122,000
International authors and editors

135M
Downloads

Our authors are among the

154
Countries delivered to

TOP 1%
most cited scientists

12.2%
Contributors from top 500 universities

CLARIVATE ANALYTICS BOOK CITATION INDEX INDEXED

WEB OF SCIENCE™

Selection of our books indexed in the Book Citation Index in Web of Science™ Core Collection (BKCI)

Interested in publishing with us?
Contact book.department@intechopen.com

Numbers displayed above are based on latest data collected.
For more information visit www.intechopen.com

2

Design and Fabrication of Miniaturized Fractal Antennas for Passive UHF RFID Tags

Ahmed M. A. Sabaawi and Kaydar M. Quboa
University of Mosul, Mosul, Iraq

1. Introduction

Generally, passive RFID tags consist of an integrated circuit (RFID chip) and an antenna. Because the passive tags are batteryless, the power transfer between the RFID's chip and the antenna is an important factor in the design. The increasing of the available power at the tag will increase the read range of the tag which is a key factor in RFID tags.

The passive RFID tag antennas cannot be taken directly from traditional antennas designed for other applications since RFID chips input impedances differ significantly from traditional input impedances of 50 Ω and 75 Ω. The designer of RFID tag antennas will face some challenges like:

- The antenna should be miniaturized to reduce the tag size and cost.
- The impedance of the designed antenna should be matched with the RFID chip input impedance to ensure maximum power transfer.
- The gain of the antenna should be relatively high to obtain high read range.

Fractal antennas gained their importance because of having interesting features like: **miniaturization**, **wideband**, **multiple resonance**, **low cost** and **reliability**. The interaction of electromagnetic waves with fractal geometries has been studied. Most fractal objects have self-similar shapes, which mean that some of their parts have the same shape as the whole object but at a different scale. The construction of many ideal fractal shapes is usually carried out by applying an infinite number of times (iteration) an iterative algorithms such as Iterated Function System (IFS).

The main focus of this chapter is devoted to design fractal antennas for passive UHF RFID tags based on traditional and newly proposed fractal geometries. The designed antennas with their simulated results like input impedance, return loss and radiation pattern will be presented. Implementations and measurements of these antennas also included and discussed.

2. Link budget in RFID systems

To calculate the power available to the reader P_r, the polarization losses are neglected and line-of-sight (LOS) communication is assumed. As shown in Fig. 1, P_r is equal to $G_r P'_r$ and can be expressed as given in equation (1) by considering the tag antenna gain G_t and the tag-reader path loss (Salama, 2010):

$$P_r = G_r P'_r = G_r P'_b \left(\frac{\lambda}{4\pi d}\right)^2 \tag{1}$$

$$= G_r G_t P_b \left(\frac{\lambda}{4\pi d}\right)^2 \tag{2}$$

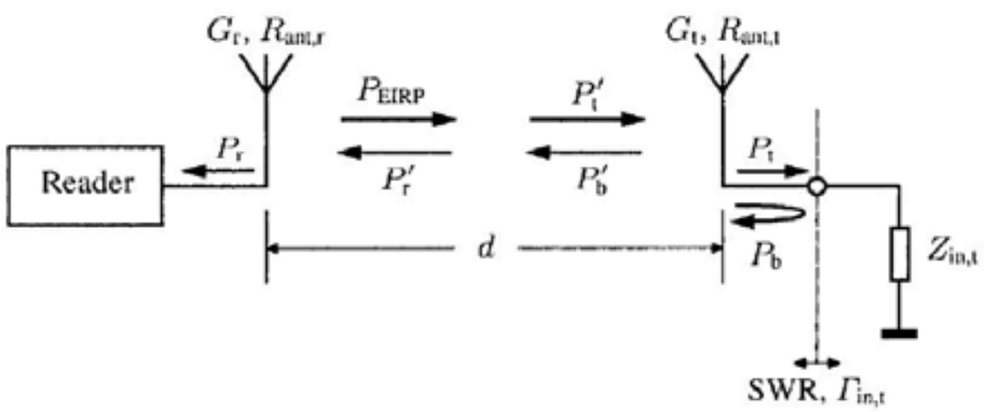

Fig. 1. Link budget calculation (Curty et al., 2007).

P'_b can be calculated using SWR between the tag antenna and the tag input impedance:

$$P_b = P_t \left(\frac{SWR - 1}{SWR + 1}\right)^2 \tag{3}$$

or can be expressed using the reflection coefficient at the interface (Γ_{in}) as:

$$P_b = P_t \left|\Gamma_{in}\right|^2 \tag{4}$$

The transmitted power (P_{EIRP}) is attenuated by reader-tag distance, and the available power at the tag is:

$$P_t G_t = P_{EIRP} \left(\frac{\lambda}{4\pi d}\right)^2 \tag{5}$$

Substituting equations (3), (4) and (5) in equation (1) will result in the link power budget equation between reader and tag.

$$P_r = G_r G_t^2 \left(\frac{\lambda}{4\pi d}\right)^4 \left(\frac{SWR - 1}{SWR + 1}\right)^2 P_{EIRP} \tag{6}$$

or can be expressed in terms of (Γ_{in}) as:

$$P_r = G_r G_t^2 \left(\frac{\lambda}{4\pi d}\right)^4 \left|\Gamma_{in}\right|^2 P_{EIRP} \tag{7}$$

The received power by the reader is proportional to the $(1/d)^4$ and the gain of the reader and tag antennas. In other words, the *Read Range* of RFID system is proportional to the fourth root of the reader transmission power P_{EIRP}.

3. Operation modes of passive RFID tags

Passive RFID tags can work in receiving mode and transmitting mode. The goals are to design the antenna to receive the maximum power at the chip from the reader's antenna and to allow the RFID antenna to send out the strongest signal.

3.1 Receiving mode

The passive tag in receiving mode is shown in Fig. 2. The RFID tag antenna is receiving signal from a reader's antenna and the signal is powering the chip in the tag.

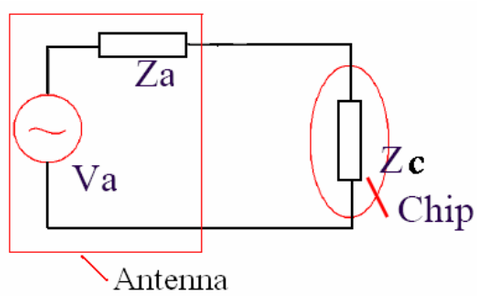

Fig. 2. Equivalent circuit of passive RFID tag at receiving mode (Salama, 2008).

where Za is antenna impedance, Zc is chip impedance and Va is the induced voltage due to receiving radiation from the reader. In this, maximum power is received when Za be the complex conjugate of Zc. In receiving mode, the chip impedance Zc is required to receive the maximum power from the equivalent voltage source Va. This received power is used to power the chip to send out radiation into the space

3.2 Transmitting mode

The passive RFID tag work in its transmitting mode as shown in Fig. 3. In transmitting mode, the chip is serving as a source and it is sending out signal thought the RFID antenna.

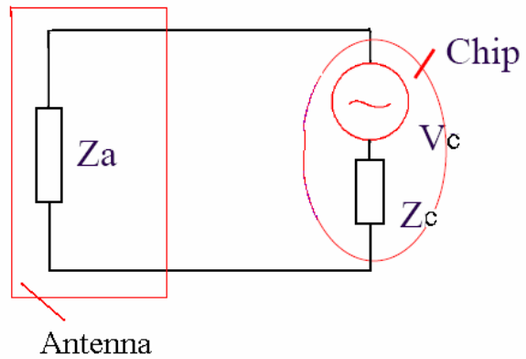

Fig. 3. Equivalent circuit of passive RFID tag in the transmitting mode (Salama, 2008).

4. Fractal antennas

A fractal is a recursively generated object having a fractional dimension. Many objects, including antennas, can be designed using the recursive nature of fractals. The term fractal, which means broken or irregular fragments, was originally coined by Mandelbrot to describe a family of complex shapes that possess an inherent self-similarity in their geometrical structure. Since the pioneering work of Mandelbrot and others, a wide variety of application for fractals continue to be found in many branches of science and engineering. One such area is fractal electrodynamics, in which fractal geometry is combined with electromagnetic theory for the purpose of investigating a new class of radiation, propagation and scatter problems. One of the most promising areas of fractal-electrodynamics research in its application to antenna theory and design (Werner et al, 1999). The interaction of electromagnetic waves with fractal geometries has been studied. Most fractal objects have self-similar shapes, which mean that some of their parts have the same shape as the whole object but at a different scale. The construction of many ideal fractal shapes is usually carried out by applying an infinite number of times (iterations) an iterative algorithms such as Iterated Function System (IFS). IFS procedure is applied to an initial structure called initiator to generate a structure called generator which replicated many times at different scales. Fractal antennas can take on various shapes and forms. For example, quarter wavelength monopole can be transformed into shorter antenna by Koch fractal. The Minkowski island fractal is used to model a loop antenna. The Sierpinski gasket can be used as a fractal monopole (Werner and Ganguly, 2003). The shape of the fractal antenna is formed by an iterative mathematical process which can be described by an (IFS) algorithm based upon a series of Affine transformations which can be described by equation (8) (Baliarda et al., 2000) (Werner and Ganguly, 2003):

$$\omega\begin{pmatrix} x \\ y \end{pmatrix} = \begin{bmatrix} r\cos\theta & -r\sin\theta \\ r\sin\theta & r\cos\theta \end{bmatrix}\begin{bmatrix} x \\ y \end{bmatrix} + \begin{bmatrix} e \\ f \end{bmatrix} \tag{8}$$

where r is a scaling factor , θ is the rotation angle, e and f are translations involved in the transformation.

Fractal antennas provide a compact, low-cost solution for a multitude of RFID applications. Because fractal antennas are small and versatile, they are ideal for creating more compact RFID equipment — both tags and readers. The compact size ultimately leads to lower cost equipment, without compromising power or read range. In this section, some fractal antennas will be described with their simulated and measured results. They are classified into two categories: 1) Fractal Dipole Antennas; which include Koch fractal curve, Sierpinski Gasket and a proposed fractal curve. 2) Fractal Loop Antennas; which include Koch Loop and some proposed fractal loops.

4.1 Fractal dipole antennas

There are many fractal geometries that can be classified as fractal dipole antennas but in this section we will focus on just some of these published designs due to space limitation.

4.1.1 Koch fractal dipole and proposed fractal dipole

Firstly, Koch curve will be studied mathematically then we will use it as a fractal dipole antenna. A standard Koch curve (with indentation angle of 60°) has been investigated

previously (Salama and Quboa, 2008a), which has a scaling factor of r = 1/3 and rotation angles of θ = 0°, 60°, -60°, and 0°. There are four basic segments that form the basis of the Koch fractal antenna. The geometric construction of the standard Koch curve is fairly simple. One starts with a straight line as an initiator as shown in Fig. 4. The initiator is partitioned into three equal parts, and the segment at the middle is replaced with two others of the same length to form an equilateral triangle. This is the first iterated version of the geometry and is called the *generator*.

The fractal shape in Fig. 4 represents the first iteration of the Koch fractal curve. From there, additional iterations of the fractal can be performed by applying the IFS approach to each segment.

It is possible to design small antenna that has the same end-to-end length of it's Euclidean counterpart, but much longer. When the size of an antenna is made much smaller than the operating wavelength, it becomes highly inefficient, and its radiation resistance decreases. The challenge is to design small and efficient antennas that have a fractal shape.

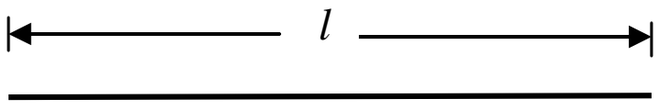

(a) Initiator

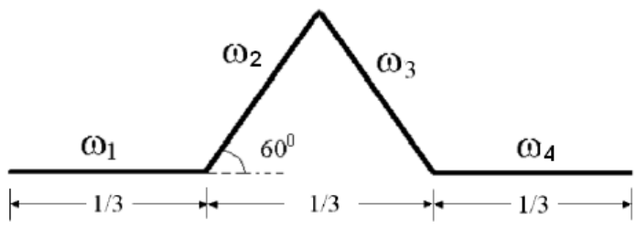

(b) Generator

Fig. 4. Initiator and generator of the standard Koch fractal curve.

Dipole antennas with arms consisting of Koch curves of different indentation angles and fractal iterations are investigated in this section. A standard Koch fractal dipole antenna using 3rd iteration curve with an indentation angle of 60° and with the feed located at the center of the geometry is shown in Fig. 5.

Fig. 5. Standard Koch fractal dipole antenna.

Table 1 summarizes the standard Koch fractal dipole antenna properties with different fractal iterations at reference port of impedance 50Ω. These dipoles are designed at resonant frequency of 900 MHz.

Indent. Angle (Deg.)	f_r (GHz)	RL (dB)	Impedance (Ω)	Gain (dBi)	Read Range (m)
20	1.86	-20	60.4-j2.6	1.25	6.08
30	1.02	-22.53	46.5-j0.6	1.18	6.05
40	0.96	-19.87	41-j0.7	1.126	6
50	0.876	-14.37	35.68+j7	0.992	5.83
60	0.806	-12.2	30.36+j0.5	0.732	5.6
70	0.727	-8.99	23.83-j1.8	0.16	5.05

Table 1. Effect of fractal iterations on dipole parameters.

The indentation angle can be used as a variable for matching the RFID antenna with specified integrated circuit (IC) impedance. Table 2 summarizes the dipole parameters with different indentation angles at 50Ω port impedance.

Iter. No.	Dim. (mm)	RL (dB)	Impedance (Ω)	Gain (dBi)	Read Range (m)
K0	127.988	-27.24	54.4-j0.95	1.39	6.22
K1	108.4 X 17	-17.56	38.4+j2.5	1.16	6
K2	96.82 X 16	-12.5	32.9+j9.5	0.88	5.72
K3	91.25 X 14	-11.56	29.1-j1.4	0.72	5.55

Table 2. Effect of indentation angle on Koch fractal dipole parameters.

Another indentation angle search between 20° and 30° is carried out for better matching. The results showed that 3rd iteration Koch fractal dipole antenna with 27.5° indentation angle has almost 50Ω impedance. This modified Koch fractal dipole antenna is shown in Fig. 6. Table 3 compares the modified Koch fractal dipole (K3-27.5°) with the standard Koch fractal dipole (K3-60°) both have resonant frequency of 900 MHz at reference port 50Ω.

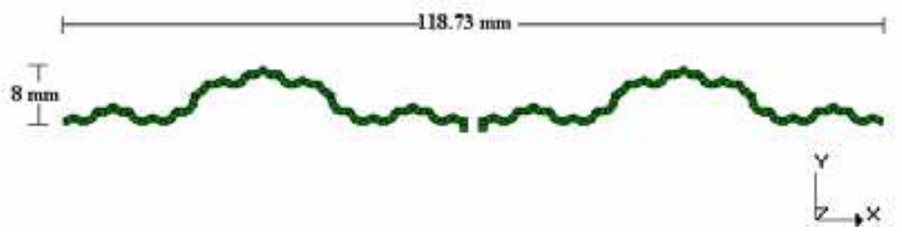

Fig. 6. The modified Koch fractal dipole antenna (K3-27.5°).

Antenna type	Dim. (mm)	RL (dB)	Impedance (Ω)	Gain (dBi)	Read Range (m)
K3-60°	91.2 X 14	-11.56	29.14-j1.4	0.72	5.55
K3-27.5°	118.7 X 8	-33.6	48+j0.48	1.28	6.14

Table 3. Comparison of (K3-27.5°) parameters with (K3-60°) at reference port 50Ω.

From Table 3, it is clear that the modified Koch dipole (K3-27.5°) has better characteristics than the standard Koch fractal dipole (K3-60°) and has longer read range.

Another fractal dipole will be investigated here which is the proposed fractal dipole (Salama and Quboa, 2008a). This fractal shape is shown in Fig. 7 which consists of five segments compared with standard Koch curve (60° indentation angle) which consists of four segments, but both have the same effective length.

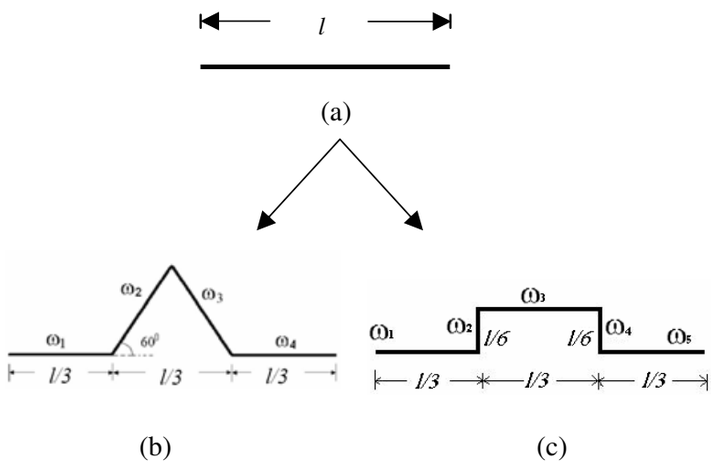

Fig. 7. First iteration of: (a) Initiator; (b) Standard Koch curve; (c) Proposed fractal curve generator .

Additional iterations are performed by applying the IFS to each segment to obtain the proposed fractal dipole antenna (P3) which is designed based on the 3rd iteration of the proposed fractal curve at a resonant frequency of 900 MHz and 50 Ω reference impedance port as shown in Fig. 8.

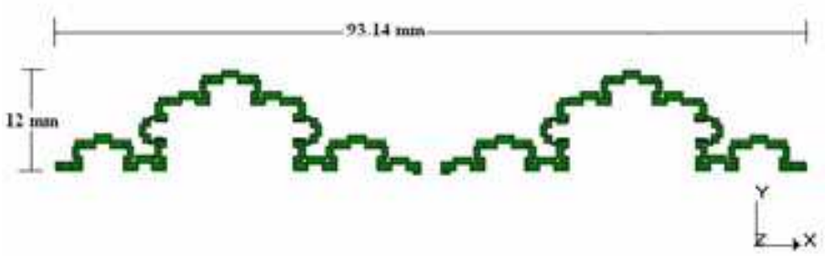

Fig. 8. The proposed fractal dipole antenna (P3) (Salama and Quboa, 2008a).

Table 4 summarizes the simulated results of P3 as well as those of the standard Koch fractal dipole antenna (K3-60°).

Antenna type	Dim. (mm)	RL (dB)	impedance (Ω)	Gain (dBi)	Read Range (m)
K3-60°	91.2 X 14	-11.56	29.14-j1.4	0.72	5.55
P3	93.1 X 12	-14.07	33.7+j3	0.57	5.55

Table 4. The simulated results of P3 compared with (K3-60°)

Fig. 9. Photograph of the fabricated K3-27.5° antenna.

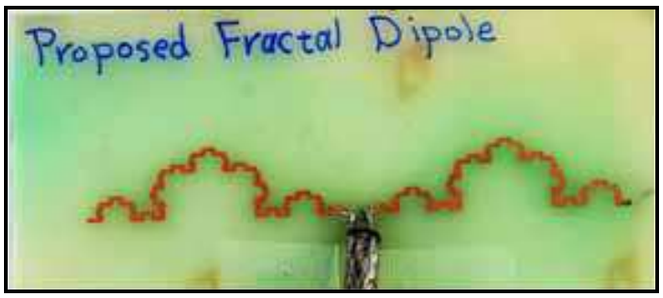

Fig. 10. Photograph of the fabricated (P3) antenna

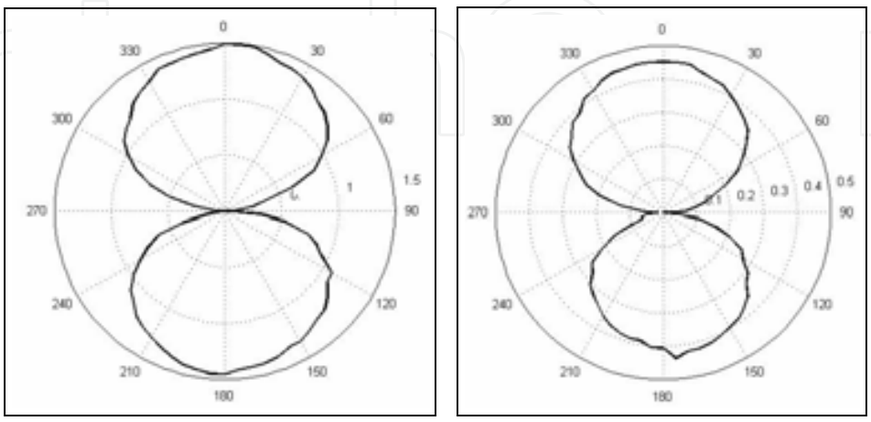

(a) (b)

Fig. 11. Measured radiation pattern of (a) (K3-27.5°) antenna and (b) (P3) antenna

These fractal dipole antennas can be fabricated using printed circuit board (PCB) technology as shown in Fig. 9 and Fig. 10 respectively. A suitable 50 Ω coaxial cable and connector are connected to those fabricated antennas. In order to obtain balanced currents, Bazooka balun may be used (Balanis, 1997). The performance of the fabricated antennas are verified by measurements. Radiation pattern and gain can be measured in anechoic chamber to obtain accurate results. The measured radiation pattern for (K3-27.5°) and (P3) fractal dipole antennas are shown in Fig. 11 which are in good agreement with the simulated results.

4.1.2 Sierpinski gasket as fractal dipoles

In this section, a standard Sierpinski gasket (with apex angle of 60°) will be investigated (Sabaawi and Quboa, 2010), which has a scaling factor of r = 0.5 and rotation angle of θ = 0°. There are three basic parts that form the basis of the Sierpinski gasket, as shown in Fig. 12. The geometric construction of the Sierpinski gasket is simple. It starts with a triangle as an initiator. The initiator is partitioned into three equal parts, each one is a triangle with half size of the original triangle. This is done by removing a triangle from the middle of the original triangle which has vertices in the middle of the original triangle sides to form three equilateral triangles. This is the first iterated version of the geometry and is called the *generator* as shown in Fig. 12.

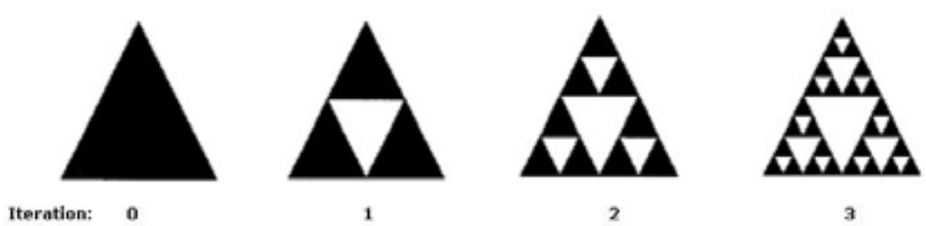

Fig. 12. The first three iterations of Sierpinski gasket.

From the IFS approach, the basis of the Sierpinski gasket can be written using equation (8).The fractal shape shown in Fig. 12 represents the first three iterations of the Sierpinski gasket. From there, additional iterations of the fractal can be performed by applying the IFS approach to each segment.

It is possible to design a small dipole antenna based on Sierpinski gasket that has the same end-to-end length than their Euclidean counterparts, but much longer. Again, when the size of an antenna is made much smaller than the operating wavelength, it becomes highly inefficient, and its radiation resistance decreases (Baliarda et al., 2000). The challenge is to design small and efficient antennas that have a fractal shape.

Dipole antennas with arms consisting of Sierpinski gasket of different apex angles and fractal iterations are simulated using IE3D full-wave electromagnetic simulator based on Methods of Moments (MoM). The dielectric substrate used in simulation has ε_r=4.1, tanδ=0.02 and thickness of (1.59) mm. A standard Sierpinski dipole antenna using 3rd iteration geometry with an apex angle of 60° and with the feed located at the center of the geometry is shown in Fig. 13.

Different standard fractal Sierpinski (apex angle 60°) dipole antennas with different fractal iterations at reference port impedance of 50 Ω are designed at resonant frequency of 900 MHz and simulated using IE3D software. The simulated results concerning Return Loss (RL), impedance, gain and read range (r) are tabulated in Table 5.

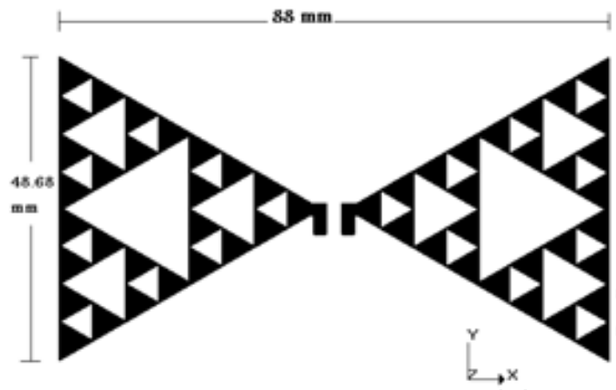

Fig. 13. The standard Sierpinski dipole antenna.

Iter. No.	Dimension (mm)	RL (dB)	Impedance (Ω)	Gain (dBi)	r (m)
0	97.66X54.3	-16.3	38.68+j7.8	1.38	6.14
1	93.6 X 51.5	-15.4	37.17+j7.5	1.32	6.08
2	89.5 X 47.5	-14	33.66+j3.22	1.25	6
3	88 X 48.68	-12.6	32.55+j8.5	1.27	5.97

Table 5. Effect of fractal iterations on standard Sierpinski dipole parameters.

It can be seen from the results given in Table 5, that the dimensions of antenna are reduced by increasing the iteration number.

In this design, the apex angle is used as a variable for matching the RFID antenna with specified IC impedance. Table 6 summarizes the dipole parameters with different apex angles. Numerical simulations are carried out to 3rd iteration Sierpinski fractal dipole antenna at 50Ω port impedance. Each dipole has a resonant frequency of 900 MHz.

Apex Angle (Deg.)	Dim. (mm)	RL (dB)	Impedance (Ω)	Gain (dBi)	r (m)
40	94.1X32.5	-15.77	36.17+j2.33	1.32	6.09
45	93.6 X 36	-15.12	35.35+j3	1.39	6.12
50	91.8X40.7	-15.34	36.61+j6.4	1.14	5.95
55	90.4X45.3	-14.84	35.21+j4.5	1.149	5.95
60	88 X 48.6	-12.6	32.55+j8.5	1.27	5.97
70	81.2X52.5	-11.8	29.83+j3.8	0.86	5.66
80	78.44X61	-9.94	26.75+j7.9	0.96	5.61

Table 6. Effect of apex angle on Sierpinski fractal dipole parameters.

From the results in Table 6, the best results (i.e. best gain and read range) are obtained at apex angle of 45°. From their, two fractal Sierpinski dipoles are designed for UHF RFID tags at 900 MHz . The first one has an apex angle of 45° (S3-45°), as shown in Fig. 14, while the other is the standard Sierpinski dipole of apex angle 60° (S3-60°).

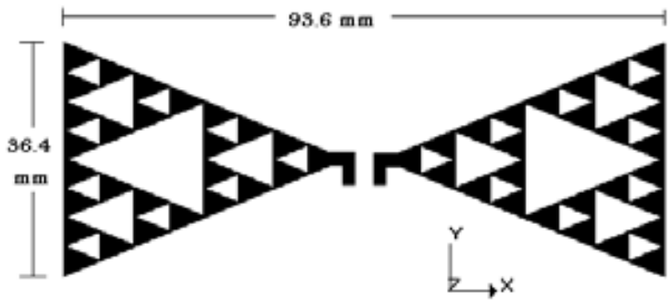

Fig. 14. The modified Seirpinski dipole antenna (S3-45°).

The effective parameters of (S3-45°) compared with the standard Sierpinski dipole (S3-60°) are given in Table 7.

Antenna type	Dim. (mm)	RL (dB)	Impedance (Ω)	Gain (dBi)	r (m)
S3-45 o	93.6 X 36	-15.1	35.35+j3	1.39	6.12
S3-60 o	88 X 48.6	-12.6	32.5+j8.5	1.27	5.97

Table 7. Comparison of (S3-45°) parameters with (S3-60°) at reference port impedance of 50Ω.

It is clear from Table 7 that the modified Sierpinski dipole antenna (S3-45°) has better gain and read range. Fig. 15 shows the simulated return loss of the modified Sierpinski dipole antenna (S3-45°).

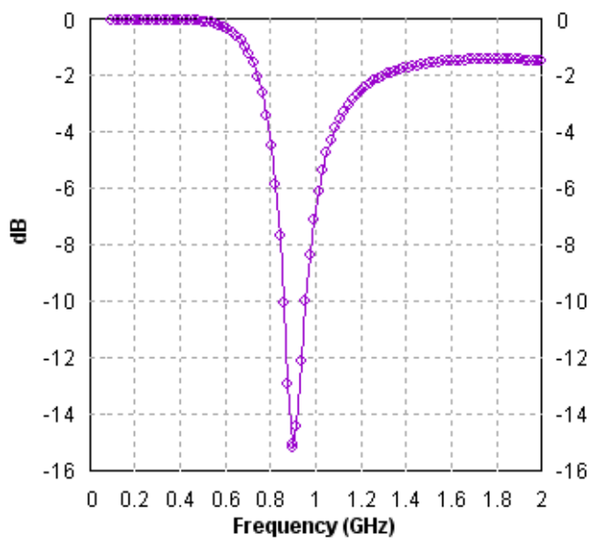

Fig. 15. The simulated return loss of (S3-45°).

The simulated radiation pattern with 2D and 3D views at φ=0 and 90° are shown in Fig. 16 for the modified Sierpinski dipole antenna (S3-45°).

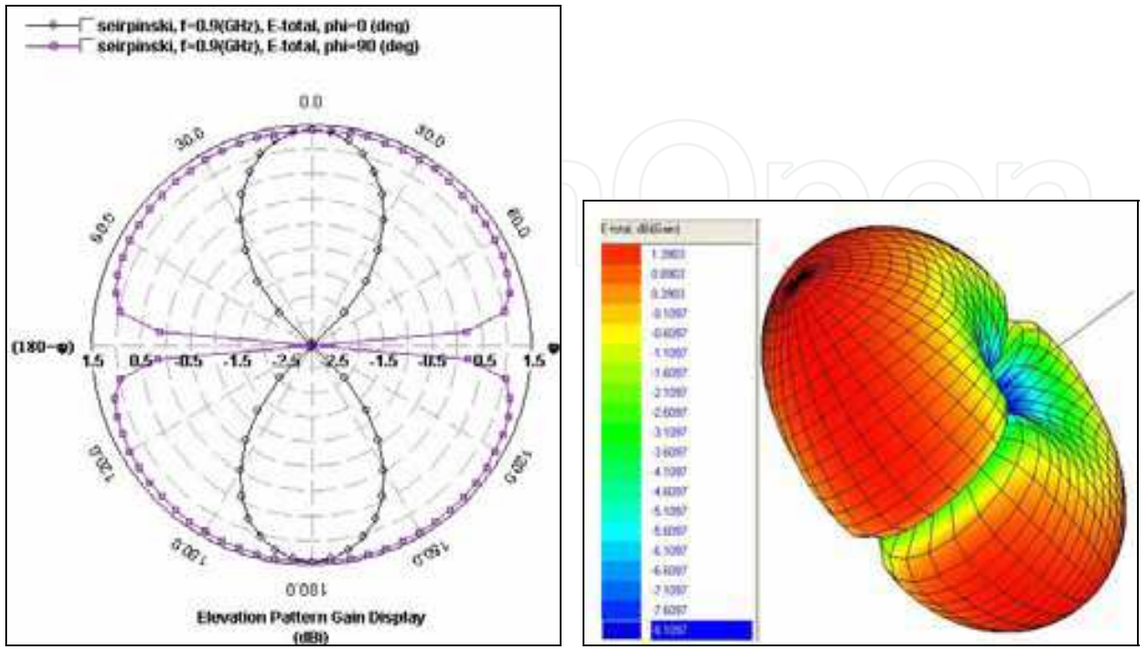

(a) (b)

Fig. 16. The simulated radiation pattern of modified Sierpinski dipole antenna (S3-45°): (a) 2D radiation pattern, (b) 3D radiation pattern.

The standard Sierpinski fractal dipole antenna (S3-60°) shown in Fig. 13 and the proposed Sierpinski fractal dipole (S3-45°) shown in Fig. 14 are fabricated using PCB technology as in Fig. 17 and Fig. 18 respectively. A 50Ω coaxial cable type RG58/U and BNC connector are connected to the fabricated antennas. In order to obtain balanced currents, Bazooka balun is used (Balanis, 1997).

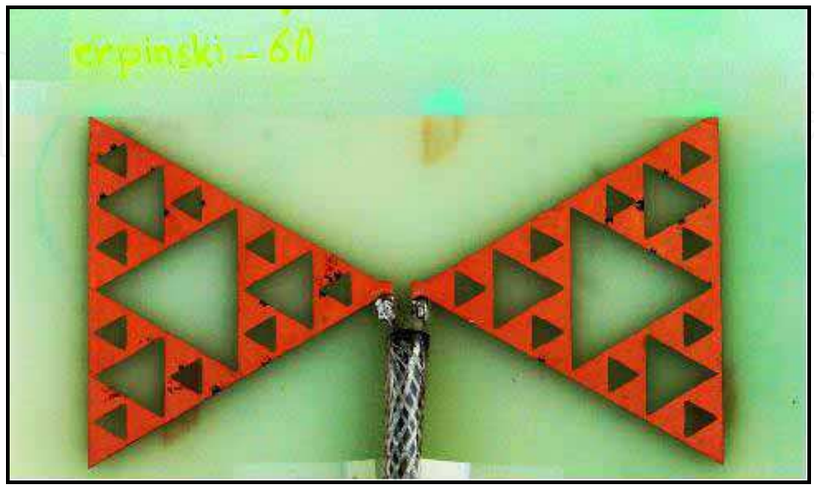

Fig. 17. The fabricated S3-60° antenna.

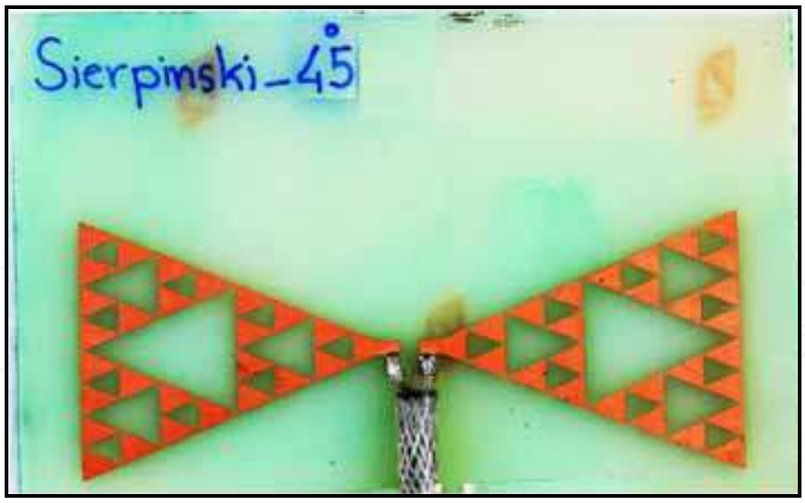

Fig. 18. The fabricated S3-45° antenna.

The performance of the fabricated antennas are verified by measurements. Radiation pattern and gain are measured in anechoic chamber. The measured radiation pattern for (S3-60°) and (S3-45°) fractal dipole antennas are shown in Fig. 19.

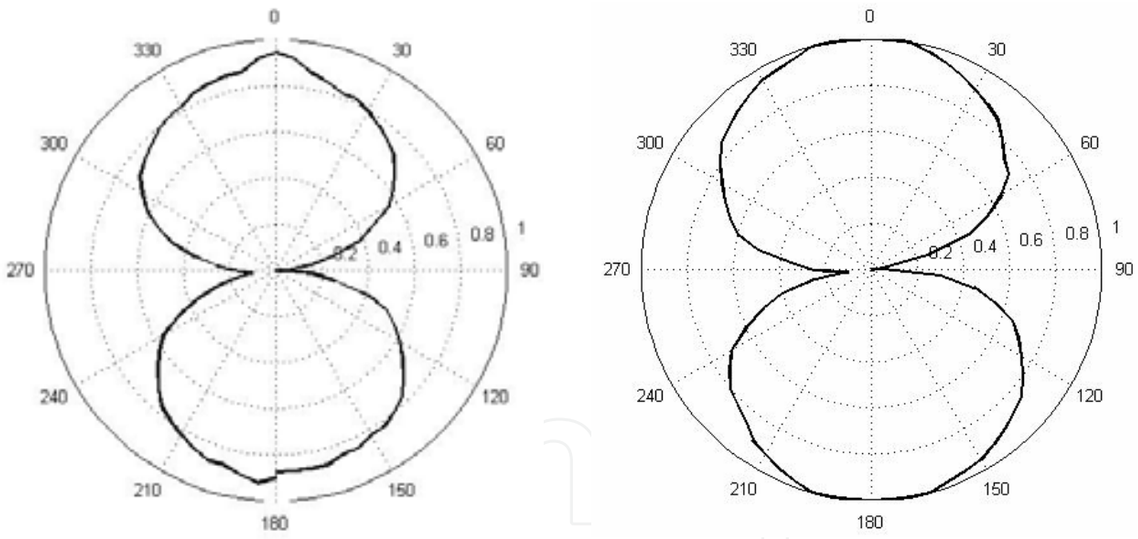

(a) (b)

Fig. 19. Measured radiation pattern for the fabricated antennas, (a) (S3-45°) antenna and (b) (S3-60°) antenna.

From Fig. 19, maximum measured gain of (0.948) dBi is obtained for (S3-45°). The measured radiation pattern was carried out for φ=0. The Return Loss of the fabricated fractal dipoles is measured using (MOTECH RF-2000) and plotted as shown in Fig. 20.

From Fig. 20, a measured RL of (-27) dB could be compared with the simulated RL of (-15.12) dB given in Table 7 for (S3-45°) while measured RL of (-27) dB is compared with simulated RL of (-12.6) dB given in Table 7 for (S3-60°).

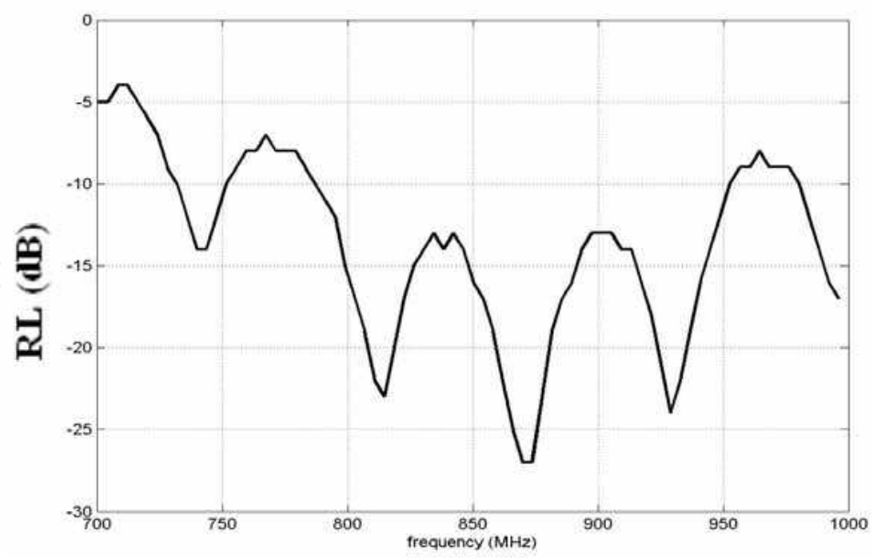

(a) Frequency (MHz)

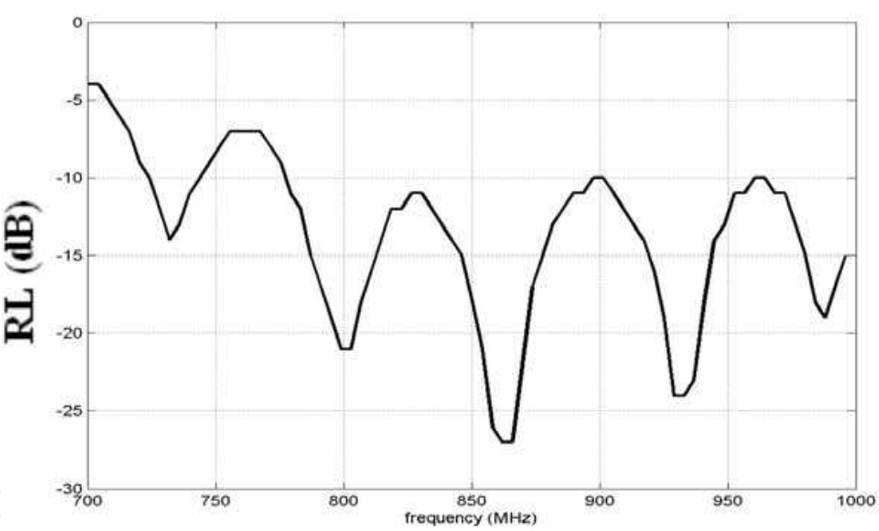

(b) Frequency (MHz)

Fig. 20. Measured RL for the fabricated antenna: (a) S3-45° antenna, (b) S3-60° antenna.

It is clear from Fig. 20 that the measured resonant frequency is around (873.86) MHz for (S3-45) and (862)MHz for (S3-60) when compared with the simulated resonant frequency at (900) MHz. The difference between measured and simulated values might be due to that the simulations are carried out using ε_r=4.1 while in practice it may be slightly different or matching was not perfect.

4.2 Fractal loop antennas

In this section, the design and performance of three fractal loop antennas for passive UHF RFID tags at 900 MHz will be investigated. The first one based on the 2nd iteration of the

Koch fractal curve and the other two loops are based on the 2nd iteration of the new proposed fractal curve with line width of (1mm) for both as shown in Fig. 21 (Salama and Quboa, 2008b).

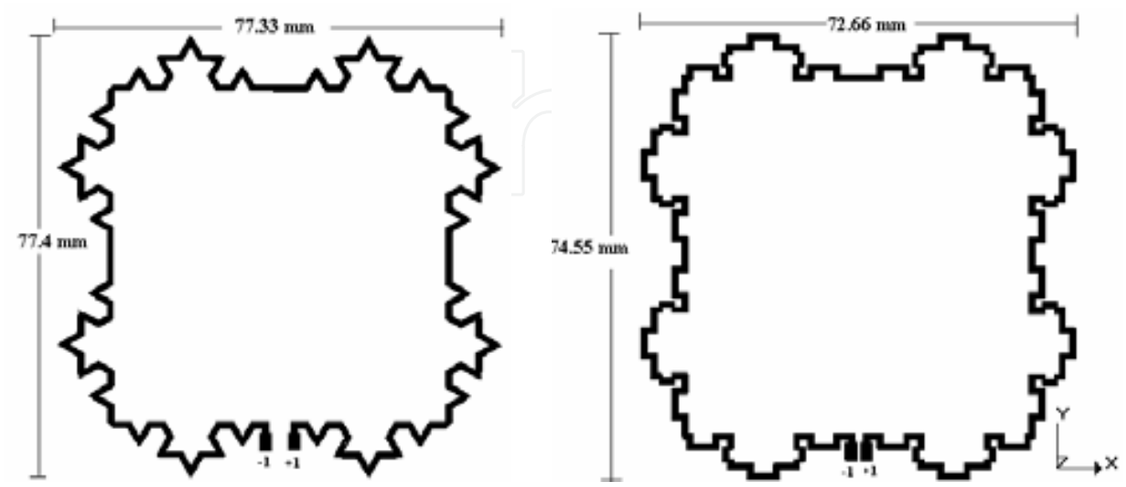

(a) (b)

Fig. 21. The designed fractal loops: (a) Standard Koch fractal loop, (b) The new proposed fractal loop

A loop antenna responds mostly to the time varying magnetic flux density $\vec{B}$ of the incident EM wave. The induced voltage across the 2- terminal's loop is proportional to time change of the magnetic flux Φ through the loop, which in turns proportional to the area *S* enclosed by the antenna. In simple form it can be expressed as (Andrenko, 2005):

$$V \propto \frac{\partial \Phi}{\partial t} \propto \omega \left| \vec{B} \right| S \tag{9}$$

The induced voltage can be increased by increasing the area (S) enclosed by the loop, and thus the read range of the tag will be increased. The proposed fractal curve has a greater area under curve than the standard Koch curve in second iteration. Starting with an initiator of length (*l*), the second iteration area is (*0.0766 l*^{2} *cm*^{2}) for the proposed curve and (*0.0688 l*^{2} *cm*^{2}) for the standard Koch curve. According to equation (9) one can except to obtain a better level of gain from proposed fractal loop higher than that from Koch fractal loop.
Fig. 22 shows the return loss (RL) of the designed loop antennas of 50Ω balanced feed port, and Table 8 summarizes the simulated results of the designed loop antennas.

Antenna type	Return Loss (dB)	BW (MHz)	Impedance (Ω)	eff. (%)	Gain (dBi)	Read Range (m)
Standard Koch Loop	-12.35	31.4	80.73-j7.3	78.5	1.74	6.287
Proposed Loop	-12.75	36	78.2-j8.9	81.8	1.97	6.477

Table 8. Simulated results of the designed loop antennas.

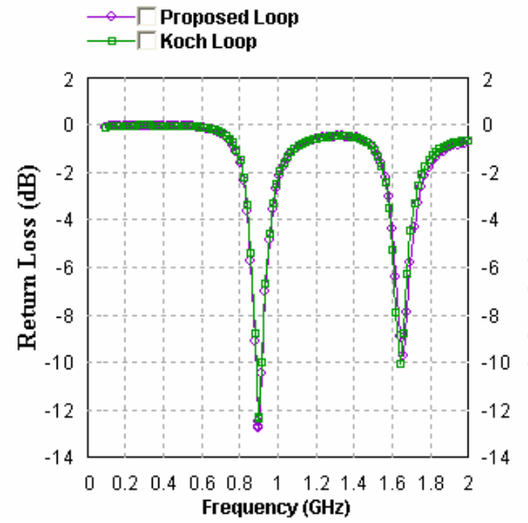

Fig. 22. Return loss of the two loop antennas.

From Table 8 it can be seen that the proposed fractal loop has better radiation characteristics than the standard Koch fractal loop. As a result, higher read range is obtained. The proposed fractal loop also is smaller in size than the standard Koch fractal loop. The measured radiation pattern is in good agreement with the simulated one for the proposed fractal loop antenna as shown in Fig. 23 .

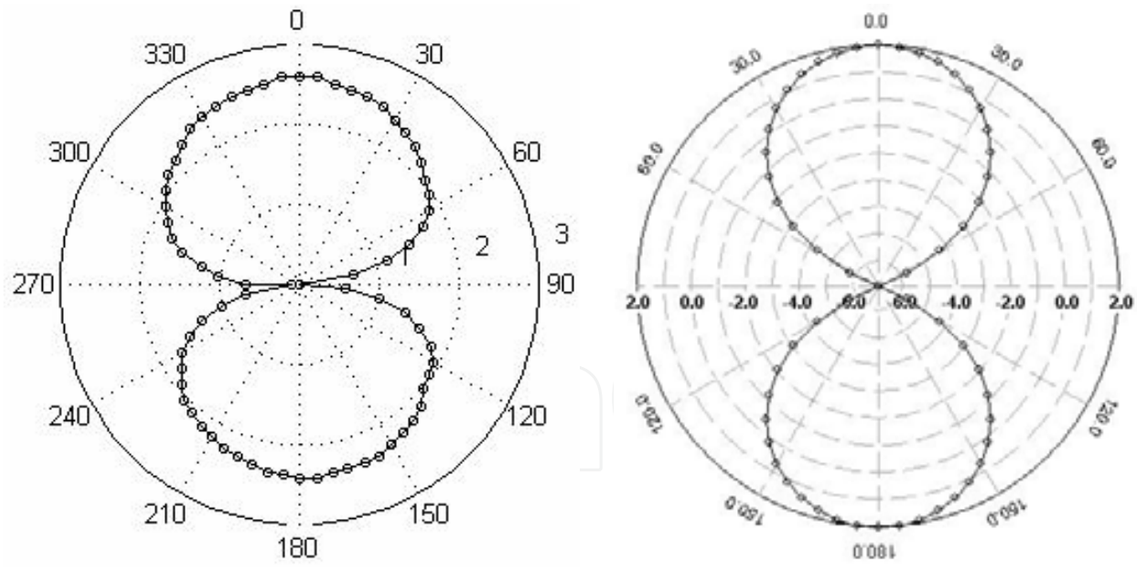

(a) (b)

Fig. 23. The radiation pattern of the proposed fractal loop antenna: (a) measured, (b) simulated (Salama& Quboa., 2008b).

Another new fractal curve is proposed as shown in Fig. 24 (Sabaawi et al, 2010) which consists of five segments compared with standard Koch curve (60° indentation angle) which consists of four segments, but has longer effective length ($l_{eff} = l \,.\, (3/2)^{n}$) compared with ($l_{eff} = l \,.\, (4/3)^{n}$) of standard Koch curve.

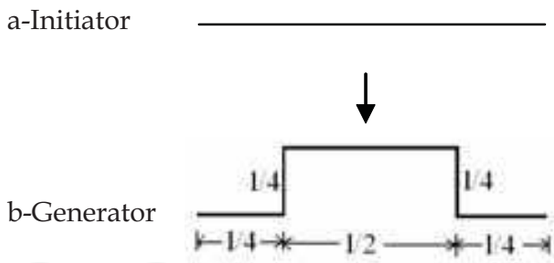

Fig. 24. First iteration of the proposed fractal curves: (a) initiator (n=0),(b) proposed fractal curve generator (n=1).

The Affine transformation of the proposed fractal curve in the ω-plane can be described according to equation (1), where θ is a rotating angle and *r* is a scaling factor, while *e* and *f* are translations involved in the transformation.

$$\omega = \left[r\cos\theta, -r\sin\theta, r\sin\theta, r\cos\theta, e, f \right] \tag{10}$$

$$\omega_1 = \left[\frac{1}{4}, 0, 0, \frac{1}{4}, 0, 0 \right]$$

$$\omega_2 = \left[0, -\frac{1}{4}, \frac{1}{4}, 0, \frac{1}{4}, 0 \right]$$

$$\omega_3 = \left[\frac{1}{2}, 0, 0, \frac{1}{2}, \frac{1}{4}, \frac{1}{4} \right]$$

$$\omega_4 = \left[0, \frac{1}{4}, -\frac{1}{4}, 0, \frac{3}{4}, \frac{1}{4} \right]$$

$$\omega_5 = \left[\frac{1}{4}, 0, 0, \frac{1}{4}, \frac{3}{4}, 0 \right]$$

$$\omega_t = \omega_1 \cup \omega_2 \cup \omega_3 \cup \omega_4 \cup \omega_5$$

Additional iterations can be performed by applying the Iterated Function System (IFS) to each segment. Fig. 25 shows the first iterations P_0, P_1, and P_2 of the proposed fractal curve.

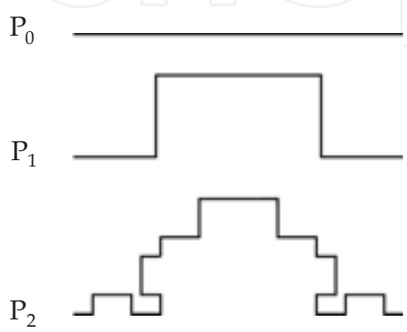

Fig. 25. First two iterations of the proposed fractal curves.

A new fractal loop antenna is designed for passive UHF RFID tags at 900 MHz based on 2nd iteration of the above proposed curve with line width of (1mm). The fractal loop is split into two halves (upper & lower halves) by making a horizontal cut at the centre of the loop as shown in Fig. 26. The central-cut is used to control the impedance of the antenna and hence increasing its matching.

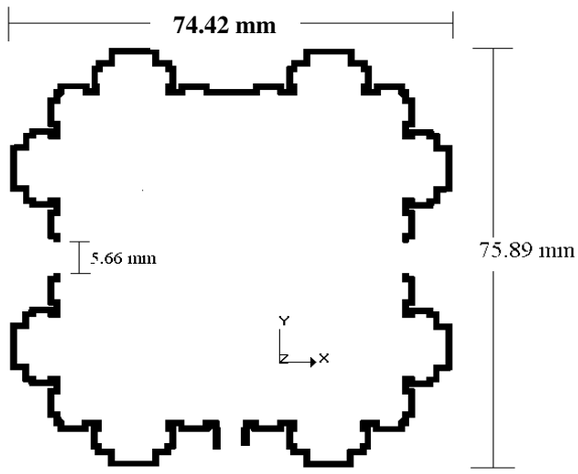

Fig. 26. The proposed fractal loop antenna.

As shown in Fig. 25, the proposed fractal curve has a greater area under curve than that of previous two loops in second iteration. Starting with an initiator of length (l), the second iterations area is ($0.1594\ l^2\ cm^2$) for the proposed curve in Fig. 26, and ($0.0766\ l^2\ cm^2$) for the fractal loop proposed in Fig. 21b (i.e more than twice the area).
The simulated results of the designed fractal loop include: input impedance (Z_a), return loss (RL) and radiation pattern will are shown in Figs. 27 & 28. These results will be useful in understanding the benefits of the designed antenna like its small size as well as its radiation properties.

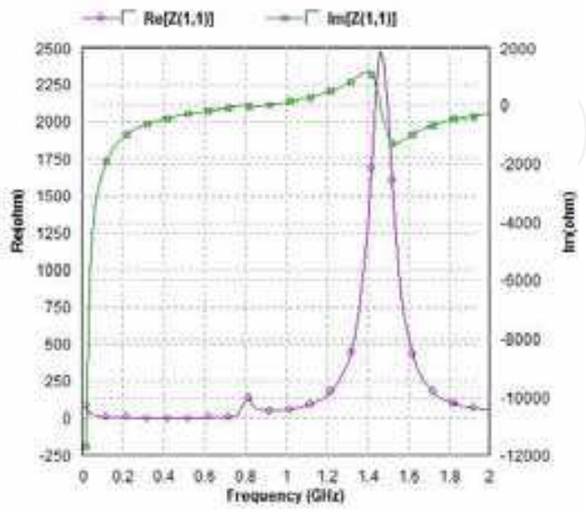

Fig. 27. The simulated input impedance of the fractal loop antenna

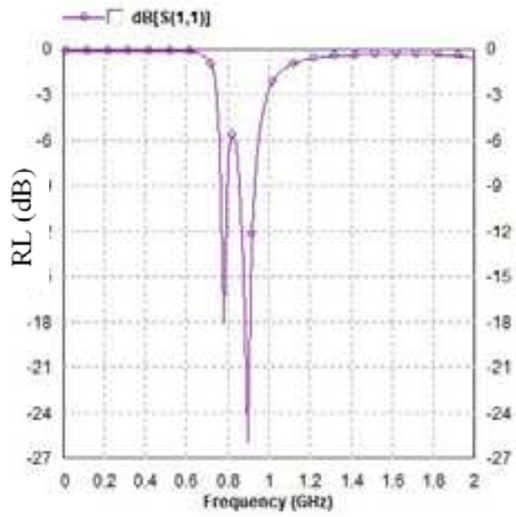

Fig. 28. The simulated return loss of the fractal loop antenna

As shown from Figs. 27 & 28, the impedance of the antenna is (65.88+j3.4) Ω at 900 MHz which is very close to the designing reference impedance of 50 Ω. It is also clear that the return loss is (-26 dB) at 900 MHz with simulated -10 dB operating bandwidth of (59 MHz). The simulated radiation pattern of the proposed fractal loop antenna is shown in Fig. 29.

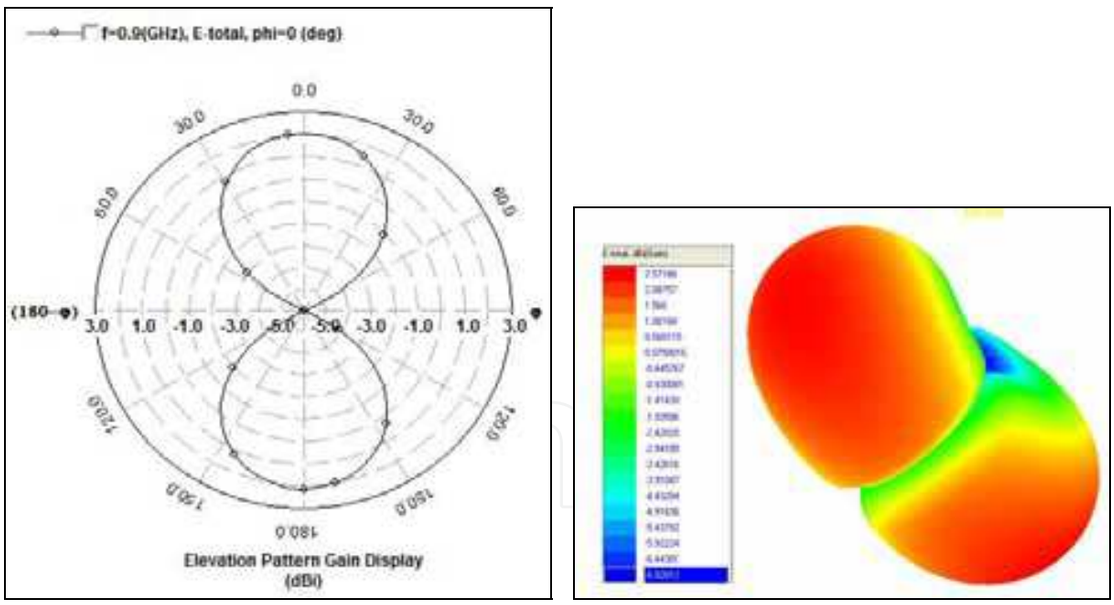

(a) (b)

Fig. 29. The simulated Radiation Pattern. (a) 2D, (b) 3D.

One can see from the Fig. 29 that the radiation pattern at 900 MHz is almost omnidirectional with deep nulls, and it is almost the same radiation pattern of an ordinary dipole with simulated gain of (2.57 dBi). Table9 summarizes the simulated results of the proposed fractal loop antenna compared with the fractal loop antenna published in (Salama and Quboa, 2008b).

Antenna type	Return Loss (dB)	BW (MHz)	Impedance (Ω)	eff. (%)	Gain (dBi)	Read Range (m)
Proposed loop	-26	59	65.8+j3.4	86.7	2.57	7.122

Table 9. Simulated characteristics of the designed fractal loop antenna.

It is clear from Table 9 that the new proposed fractal loop has better radiation characteristics from all those of the proposed fractal loop in (Salama and Quboa, 2008b) under the same design conditions and parameters (i.e. the same substrate parameters), and as a result longer read range is obtained which is the most important factor in designing RFID tags.
The proposed fractal loop antenna shown in Fig. 26 is fabricated using PCB technology as shown in Fig. 27. A 50Ω coaxial cable type RG58/U and BNC connector is connected to the fabricated antenna. In order to obtain balanced currents, Bazooka balun is used. The performance of the fabricated antennas is verified by measurements. Radiation pattern is measured in anechoic chamber. The return loss of the fabricated loop antenna is measured using MOTECH RF-2000 analyzer as shown in Fig. 28.

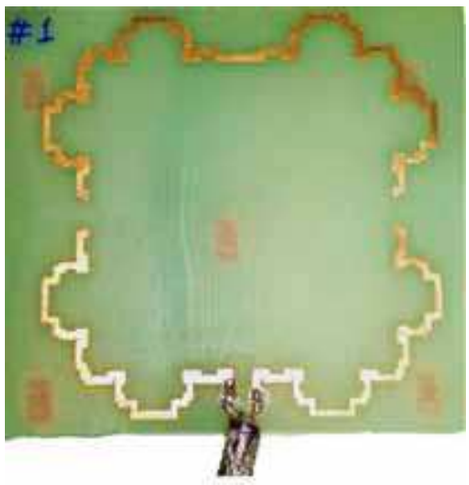

Fig. 27. The Fabricated Fractal Loop Antenna.

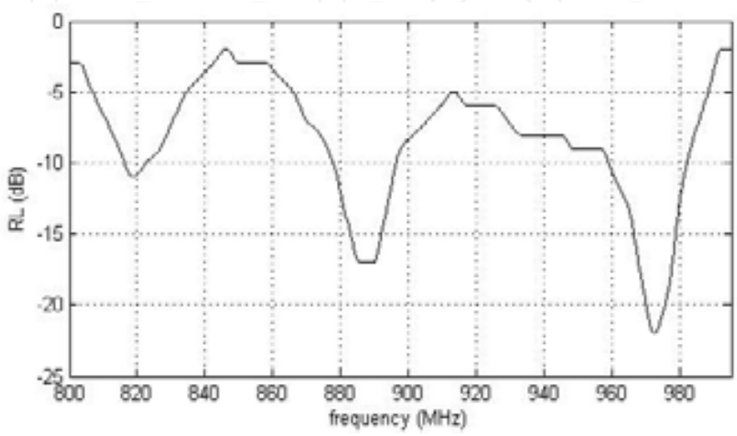

Fig. 28. Measured RL of the fabricated fractal loop antenna.

The measured return loss is (-17 dB) at a resonant frequency (889.62 MHz) compared with the simulated one of (-26 dB) at 900 MHz, and the bandwidth is (19.2 MHz) compared with the simulated bandwidth of (59 MHz). The disagreement between measured and simulated results of the fractal loop antenna is attributed to the fact that we lack sufficient information from the vendor of FR-4 material. This information would enable us to build accurate model for the dielectric material in the EM simulator, instead of working with single frequency point data.

The radiation pattern for the fractal dipole antenna is measured in anechoic chamber as shown in Fig. 29 which is in good agreement with the simulated results.

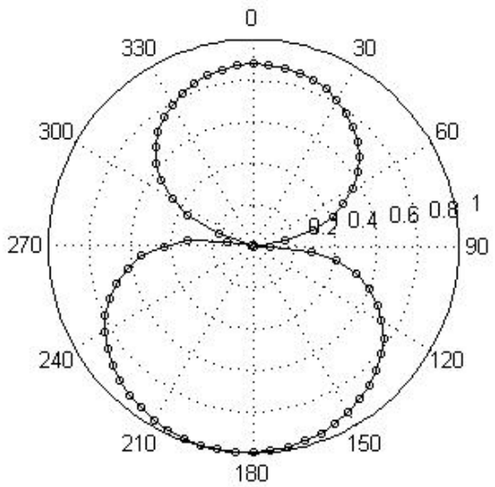

Fig. 29. Measured radiation pattern.

5. References

Andrenko A. S., (2005). Conformal Fractal Loop Antennas for RFID Tag Applications, *Proceedings of the IEEE International Conference on Applied Electromagnetics and Communications, ICECom.*, Pages:1-6, Oct. 2008.

Balanis C. A., (1997), Antenna Theory Analysis and Design, Jhon Whily, New York, (2nd Edition).

Baliarda C. P., Romeu J., & Cardama A., M. (2000), The Koch monopole: A small fractal antenna. *IEEE Trans. on Antennas and Propagation,* Vol.48, (2000) page numbers (1773-1781).

Curty J. P., Declerdq M., Dehollain C. & Joehl N. , (2007). *Design and Optimization of Passive UHF RFID Systems,* Springer, ISBN: 0-387-35274-0, New Jersey.

Sabaawi A. M. A., Abdulla A. I., Sultan Q. H., (2010), Design a New Fractal Loop Antenna For UHF RFID Tags Based On a Proposed Fractal Curve, Proceedings of The 2nd IEEE International Conference on Computer Technology and Development (ICCTD 2010) November 2-4, 2010, Cairo, Egypt.

Sabaawi A. M. A., Quboa K. M., (2010). Sierpinski Gasket as Fractal Dipole Antennas for Passive UHF RFID Tags. Proceedings of The Mosharaka International Conference on Communications, Electronics, Propagation (MIC-CPE2010), 3-5 March 2010, Amman, Jordan.

Salama A. M. A., (2010). Antennas of RFID Tags, Radio Frequency Identification Fundamentals and Applications Design Methods and Solutions, Cristina Turcu (Ed.), ISBN: 978-953-7619-72-5, INTECH, Available from: http://sciyo.com/articles/show/title/antennas-of-rfid-tags.

Salama A. M. A., Quboa K., (2008a). Fractal Dipoles As Meander Lines Antennas For Passive UHF RFID Tags, *Proceedings of The IEEE Fifth International Multi-Conference on Systems, Signals and Devices (IEEE SSD'08)*, Page: 128, Jordan, July 2008.

Salama A. M. A., Quboa K., (2008b). A New Fractal Loop Antenna for Passive UHF RFID Tags Applications, *Proceedings of the 3rd IEEE International Conference on Information & Communication Technologies: from Theory to Applications (ICTTA'08)*, Page: 477, Syria, April 2008, Damascus.

Werner D. H. & Ganguly S. (2003). An Overview of Fractal Antenna Engineering Research. *IEEE Antennas and Propagation Magazine,* Vol.45, No.1, (Feb. 2003), page numbers (38-56).

Werner D. H., Haupt R. L., Werner P. L., (1999). Fractal Antenna Engineering: The Theory and Design of Fractal Antenna Arrays. *IEEE Antennas and Propagation Magazine,* Vol.41, No.5, (1999) ,page numbers (37-58).

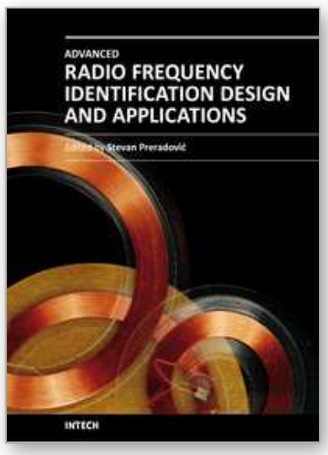

Advanced Radio Frequency Identification Design and Applications

Edited by Dr Stevan Preradovic

ISBN 978-953-307-168-8
Hard cover, 282 pages
Publisher InTech
Published online 22, March, 2011
Published in print edition March, 2011

Radio Frequency Identification (RFID) is a modern wireless data transmission and reception technique for applications including automatic identification, asset tracking and security surveillance. This book focuses on the advances in RFID tag antenna and ASIC design, novel chipless RFID tag design, security protocol enhancements along with some novel applications of RFID.

How to reference

In order to correctly reference this scholarly work, feel free to copy and paste the following:

Ahmed M. A. Sabaawi and Kaydar M. Quboa (2011). Design and Fabrication of Miniaturized Fractal Antennas for Passive UHF RFID Tags, Advanced Radio Frequency Identification Design and Applications, Dr Stevan Preradovic (Ed.), ISBN: 978-953-307-168-8, InTech, Available from: http://www.intechopen.com/books/advanced-radio-frequency-identification-design-and-applications/design-and-fabrication-of-miniaturized-fractal-antennas-for-passive-uhf-rfid-tags

INTECH
open science | open minds

InTech Europe
University Campus STeP Ri
Slavka Krautzeka 83/A
51000 Rijeka, Croatia
Phone: +385 (51) 770 447
Fax: +385 (51) 686 166
www.intechopen.com

InTech China
Unit 405, Office Block, Hotel Equatorial Shanghai
No.65, Yan An Road (West), Shanghai, 200040, China
中国上海市延安西路65号上海国际贵都大饭店办公楼405单元
Phone: +86-21-62489820
Fax: +86-21-62489821

IntechOpen